

Characterization of GaAs_{1-x}N_x epitaxial layers by ion beam analysis

P. Wei,^{a)} M. Chicoine, S. Gujrathi, and F. Schiettekatte

Groupe de recherche en physique et technologie des couches minces, Lab. René-J.-A. Lévêque, Département de Physique, Université de Montréal, P.O. Box 6128, Station Centre-ville, Montréal, Québec H3C 3J7, Canada

J.-N. Beaudry, R. A. Masut, and P. Desjardins

Groupe de recherche en physique et technologie des couches minces, Département de Génie Physique, École Polytechnique de Montréal, P.O. Box 6079, Station Centre-ville, Montréal, Québec H3C 3A7, Canada

(Received 12 September 2003; accepted 22 December 2003; published 18 May 2004)

GaAs_{1-x}N_x epitaxial layers grown on (001) GaAs substrates by metal organic vapor phase epitaxy, with x ranging from 0.01 to 0.036, were characterized by ion beam analysis. The layers thickness and quality were measured by Rutherford backscattering spectrometry (RBS) in channeling mode. The channeling results confirm that GaAs_{1-x}N_x epitaxial layers are of high crystalline quality, in agreement with high resolution x-ray diffraction and transmission electron microscopy analyses. For the sample with $x=0.036$, the results reveal a 0.7 at. % of misplaced (or highly locally strained) Ga or As atoms. More than 80% of nitrogen atoms in this layer occupy substitutional sites, as determined by the ¹⁴N(α ,p)¹⁷O nuclear reaction analysis (NRA). Furthermore, RBS analyses using a 5 MeV O³⁺ probe beam reveal measurable departures from III-V stoichiometry near the surface, which remains unexplained. Finally, the total content of nitrogen in the layers measured both by NRA and elastic recoil detection by time-of-flight are compared with the results obtained by secondary ion mass spectrometry. © 2004 American Vacuum Society. [DOI: 10.1116/1.1648671]

I. INTRODUCTION

The strong dependence of the band gap on the N content has made diluted GaAs_xN_{1-x} a promising material for a variety of applications such as long wavelength optoelectronic devices and high efficiency hybrid solar cells.¹ The large N-As size difference translates into a predicted limited miscibility on the anion sublattice, leading to the formation of phase separation induced alloy nanostructure. Up to now, it has been possible to substitutionally incorporate only a few atomic percent nitrogen in GaAs by molecular beam epitaxy,^{2,3} and metal organic vapor phase epitaxy (MOVPE).^{4,5}

It is crucial to know the total N fraction as well as the precise lattice configurations in the epitaxial layer not only from an application point of view, but also to better understand and control the fundamental growth mechanisms. By properly selecting the different ion beam analysis methods, such as Rutherford backscattering spectrometry (RBS), nuclear reaction analysis (NRA), and elastic recoil detection (ERD),^{6,7} all of the elements, light or heavy, in the sample, can be characterized with a reasonable sensitivity.

In this article, RBS in channeling mode (RBS/channeling) and NRA using ¹⁴N(α ,p)¹⁷O endothermic nuclear reaction were applied to characterize GaAs_xN_{1-x} epitaxial layers grown on (001) GaAs substrates by MOVPE with x varying from 0.01 to 0.036, as characterized by secondary ion mass spectrometry (SIMS).⁸ The quality and, in some particular cases, the thickness of the layer can be measured by RBS/channeling. The relative concentrations of Ga and As in the surface region were further obtained using 5 MeV O⁺ heavy

ion RBS measurement. The total content of nitrogen and the fraction of substitutional nitrogen were quantified by NRA and ERD with a time-of-flight detector (ERD-TOF).

II. EXPERIMENT

GaAs_xN_{1-x} epitaxial layers were grown on semi-insulating GaAs (001) substrates in a cold wall MOVPE reactor using trimethylgallium, tertiarybutylarsine, and 1,1-dimethylhydrazine precursors for Ga, As, and N, respectively. Details of the samples preparation can be found elsewhere.⁸ Four samples with x ranging from 0.01–0.036, as listed in Table I, were characterized by ion beam analysis.

Ion beam analyses were carried out on the 1.7 and 6 MV tandem accelerators at Université de Montréal. Samples were mounted on a computer-controlled stepping motor driven three-axes goniometer with a precision of $\pm 0.01^\circ$. A 200 V voltage was applied on the sample holder to suppress secondary electron emission. A 360° movable passivated implanted planar silicon detector was located at 170° for RBS measurements and 160° for NRA detection, respectively. The current on the target was also monitored by prior and subsequent current measurements in a Faraday cup, confirming that the beam intensity was stable throughout the experiments.

RBS/channeling experiments were performed using a 2 MeV He⁺ beam with a current of about 3 nA. RBS spectra in the random and aligned along $\langle 100 \rangle$ and $\langle 110 \rangle$ directions were collected for each sample.

Several nuclear reactions can be used to characterize nitrogen, including ¹⁴N(d, α)¹²C, ¹⁴N(d,p)¹⁵N, and ¹⁴N(d, γ)¹⁸F. However deuterium beam activation will induce long-term radiation background in the setup. Instead,

^{a)}Electronic mail: peng.wei@UMontreal.CA

TABLE I. Nitrogen fraction of element V sublattice sites in the GaAs_{1-x}N_x epilayers measured by NRA, ERD-TOF, compared to SIMS values.⁸

| Sample | NRA | ERD-TOF | SIMS |
|--------|-------------|-------------|-------------|
| No. 41 | 0.034±0.006 | 0.032±0.005 | 0.036±0.004 |
| No. 46 | 0.027±0.006 | | 0.024±0.002 |
| No. 59 | 0.010±0.003 | 0.022±0.002 | 0.025±0.002 |
| No. 18 | 0.005±0.003 | 0.006±0.001 | 0.012±0.001 |

the ¹⁴N(α ,p)¹⁷O endothermic resonance nuclear reaction was chosen, using a resonance energy of 3.72 MeV He²⁺ beam,^{9,10} which produces 1.23 MeV protons. Six layers of 2.54 μ m mylar foil with a total thickness of 15.24 μ m were placed in front of the detector to stop the elastically scattered α particles. The total collected charge for each sample was 100 μ C with a beam current of about 20 nA in order to get sufficient statistics while keeping beam-induced damage negligible. In order to quantify the total content of nitrogen in the sample, a thick kapton foil with a known N concentration was measured as a reference under the same experimental conditions. For the detection of N in the channeling geometry, the sample was first aligned along the $\langle 100 \rangle$ direction using 2 MeV He⁺ without the stopping foil in front of the detector.

The composition of Ga and As in the epitaxial layer was explored by heavy ion Rutherford backscattering spectrometry (HIRBS) using a 5 MeV O³⁺ beam for which the mass resolution is greatly improved and the surface signal from Ga and As can be separated and therefore easily quantified. Finally, the total N and other light elements contents were also measured by elastic recoil detection with a time-of-flight detector (ERD-TOF) using a 50 MeV Cu⁹⁺ beam.¹¹ In our setup, however, this technique cannot be used in channeling mode.

III. RESULTS AND DISCUSSION

Figure 1 shows the RBS spectra of sample No. 41 collected in random, $\langle 100 \rangle$ and $\langle 110 \rangle$ directions. The estimation of χ_{\min} , obtained by comparing the $\langle 100 \rangle$ channeling and random spectra, is $\sim 7\%$, which demonstrates the good quality of the epitaxial layer. This is in agreement with results obtained by high resolution x-ray diffraction (HR-XRD) and transmission electron microscopy analyses.⁸ Looking closely at the channeling spectra that were enlarged in the inset of Fig. 1, we find that the aligned GaAs yield in the layer region is higher than that in the substrate region along the $\langle 100 \rangle$ direction while the reverse phenomenon is observed along the $\langle 110 \rangle$ direction. The steps are due to the difference between the layer and the substrate. Therefore, the thickness of the layer can be obtained by simulating the portion above the energy of the step edge in the RBS/channeling spectra, assuming that the stopping powers are the same as in the random direction based on the Aarhus convention.¹² In the case of the sample shown in Fig. 1, the thickness found is 180 ± 5 nm, in good agreement with the value of 184 nm found by a combination of SIMS and Dektak profilometry. More importantly, the higher yield observed in the layer region along the

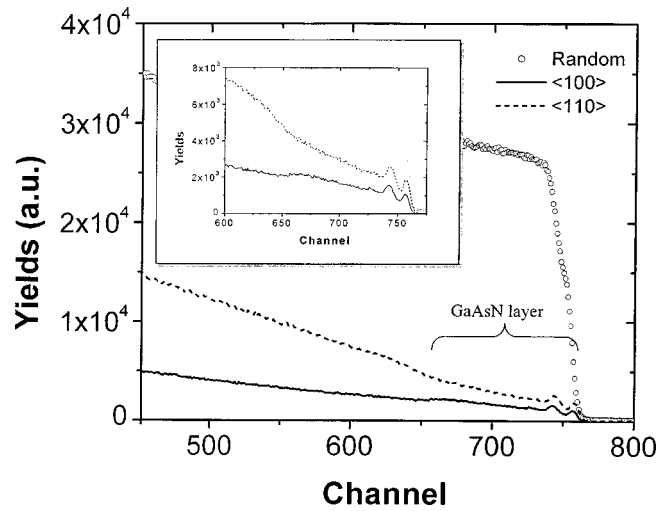


Fig. 1. RBS/channeling spectra obtained along the $\langle 100 \rangle$ and the $\langle 110 \rangle$ directions as well as in the random direction for sample No. 41; the inset shows an enlarged portion of spectra.

$\langle 100 \rangle$ direction is a clear signature of the presence of misplaced Ga and/or As atoms in the layer, such as interstitials or defect clusters.

In the $\langle 110 \rangle$ channeling direction, the step edge observed at the layer/substrate interface is due to the lattice strain induced by the incorporation of nitrogen atoms. A similar effect is also observed along the $\langle 111 \rangle$ direction. This edge could also hide the presence of misplaced atoms otherwise detectable in this direction. From the height of the bump along the $\langle 100 \rangle$ channel, after subtraction from the dechanneling contribution, an estimate indicates that the concentration of misplaced atoms should be of the order of 0.7% in this sample with a total N fraction of 0.034 obtained later by NRA. Interstitials located at $(1/2, 1/2, 1/2)$ are excluded since they would not be detectable along this direction.

This higher yield could also be due to high local strain caused by substitutional N atoms on the four neighboring Ga atoms. Given the amount of N in this sample, 14% of the Ga atoms are nearest neighbor of N atoms, which would result in a network of oddly strained atoms. However, unless the total displacement of the atoms is very large, strain should only contribute to a dechanneling effect on the beam, and not to a bump in the yield along the $\langle 100 \rangle$ direction.

While HR-XRD measurements reveal that samples with a N content smaller than $x=0.03$ follow closely the Vegard rule of substitutional incorporation of N, a departure from this rule is observed for samples with higher N content, with a lattice constant decreasing even more rapidly than for substitutional incorporation. The departure reaches 20% for sample with $x=0.036$. It thus seems that the features observed in channeling are a result of the phenomenon responsible for Vegard's rule departure since they were not observed in samples with lower N concentrations.

Figure 2 presents the HIRBS spectra from the same sample as well as from a pure GaAs layer, and the related RUMP simulations.¹³ The use of a heavier ion together with a more energetic probe beam results in much

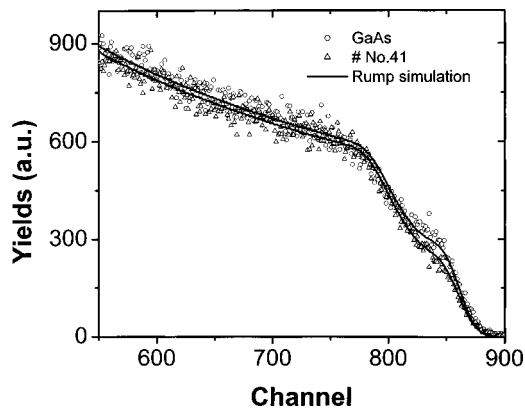


FIG. 2. HIRBS spectrum using 5 MeV O⁺ beam, circles: pure GaAs; triangles: Sample No. 41; lines: RUMP simulation.

better mass separation for Ga and As atoms compared to RBS measurements with a conventional 2 MeV He beam (Fig. 1). This allows for a precise determination of the surface composition of As and Ga in the samples. While HIRBS offers poorer energy resolution in this case, the depth resolution is similar to RBS with a MeV He beam considering the higher stopping power of O in GaAs. The simulated results indicate that the concentration near the surface is GaAs_{0.90±0.03}. The reason for As deficit is not known. Further ERD-TOF measurement, HIRBS/channeling experiments and x-ray photoelectron spectrometry will be carried out to shed light on the interaction between N, O, C, Ga, and As atoms.

Figure 3 shows the NRA spectra from the sample No. 41 along $\langle 100 \rangle$ and random directions. The quantitative concentration of nitrogen was extracted by a relative measurement using a thick kapton foil as a reference for nitrogen. By comparing the maximum yields of the peak around channel 260 in Fig. 3, χ_{\min} is about 18%. Taking into account that χ_{\min} for GaAs is $\sim 7\%$, the fraction of substitutional nitrogen can be estimated by the following expression: $[1 - \chi_{\min}(\text{NRA})]/(1 - \chi_{\min}(\text{RBS})]$, in this case 88% of the to-

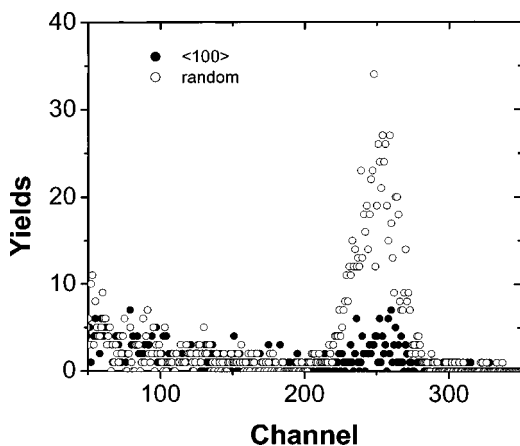


FIG. 3. Nuclear reaction analysis spectra obtained along the $\langle 100 \rangle$ and the random directions for sample No. 41, using the $^{14}\text{N}(\alpha, p)^{17}\text{O}$ endothermic reaction.

tal nitrogen in this sample. The total N content, measured by NRA in the random direction, is 3.4%, very close to the value of $3.6 \pm 0.3\%$ measured by SIMS.⁸ Thus the concentration of misplaced N is around 0.6%. This value is in good agreement with the estimated concentration of misplaced atoms $\sim 0.7\%$ found from the bump in the spectrum measured along the $\langle 100 \rangle$ direction in Fig. 1, indicating similar amounts of N and Ga/As misplaced atoms. This suggests that they are involved in a defect complex. The presence of Ga-N split-interstitials has to be ruled out, however, as the associated compressive strain would compensate for the tensile strain due to substitutional N. We know from HR-XRD measurements that the magnitude of the tensile strain increases beyond Vegard's rule for N concentration above 3%. It is thus clear from current results that more complex defect structures are involved. Further characterization by other methods as well as simulations of the channeling spectra need to be carried out in order to draw further conclusions about the nature of the non-substitutional N.

Finally, Table I shows the N content we have measured in several GaAs_{1-x}N_x layers obtained by NRA and ERD-TOF, compared to the SIMS measurements.⁸ For the samples with high N content, the NRA results are very close to the SIMS values while samples with lower N content show a larger discrepancy. ERD-TOF measurements confirmed the concentration measured by SIMS and NRA for the sample with the highest N content. For the two samples with a lower N content, ERD-TOF is closer to the SIMS results for sample No. 59, but corroborates the NRA result for sample No. 18, which has the smaller amount of N. The reason for this discrepancy is not clear at the moment, but it is worth mentioning that a small number of detected atoms was obtained from these samples. The error estimates reflect the statistical uncertainty on these values. Although ERD-TOF may be the best choice for detecting light elements in the heavier target since it does not require any standard, the advantages of NRA are that it can be used for channeling measurements at normal incidence, and that less radiation damage is induced by the analyzing beam. Compared with SIMS, it is a non-destructive technique for quantitative characterization of layers, also providing information on atomic location. If an accurate nuclear reaction cross section is available, an absolute analysis can be carried out without using any reference sample.

IV. SUMMARY

GaAs_{1-x}N_x samples were characterized by RBS/channeling, HIRBS NRA, and ERD-TOF ion beam analysis. For the sample with $x = 0.036$, the results confirm that high quality strained epitaxial layers were grown. Based on the NRA results on the random and channeling geometries, more than 80% of nitrogen atoms in this epilayer occupy substitutional sites of the zinc-blende lattice. HIRBS analysis reveals that less As atoms than Ga atoms were incorporated in the surface region of the layer. Channeling in the $\langle 100 \rangle$ direction also show the presence of a fair amount of Ga or As displaced in the layer, at a concentration equivalent to the amount of interstitial N atoms. Further characterization and

simulations need to be carried out in order to identify the structure of the defect complexes present in these samples.

ACKNOWLEDGMENTS

The authors acknowledge R. Gosselin and L. Godbout for their technical assistance. This work was supported by the Natural Science and Engineering Council of Canada (NSERC) and NanoQuébec.

- ¹I. A. Buyanova, W. M. Chen, and B. Monemar, *MRS Internet J. Nitride Semicond. Res.* **6**, 1 (2001).
- ²S. Z. Wang, S. F. Yoon, W. K. Loke, T. K. Ng, and W. J. Fan, *J. Vac. Sci. Technol. B* **20**, 1364 (2002).
- ³A. R. Kovsh, J. S. Wang, L. Wei, R. S. Shiao, J. Y. Chi, B. V. Volovik, A. F. Tsatsul'nikov, and V. M. Ustinov, *J. Vac. Sci. Technol. B* **20**, 1158 (2002).
- ⁴B. F. Moody, P. T. Barletta, N. A. El-Masry, J. C. Roberts, M. E. Aumer, S. F. LeBoeuf, and S. M. Bedair, *Appl. Phys. Lett.* **80**, 2475 (2002).

- ⁵H. Dumont, L. Auvray, Y. Monteil, C. Bondoux, L. Largeau, and G. Patriarche, *Appl. Phys. Lett.* **80**, 2460 (2002).
- ⁶T. Ahlgren, E. Vainonen-Ahlgren, J. Likonen, W. Li, and M. Pessa, *Appl. Phys. Lett.* **80**, 2314 (2002).
- ⁷W. Li, M. Pessa, T. Ahlgren, and J. Decker, *Appl. Phys. Lett.* **79**, 1094 (2001).
- ⁸J.-N. Beaudry, R. A. Masut, P. Desjardins, P. Wei, M. Chicoine, G. Bentoumi, R. Leonelli, F. Schiettekatte, and S. Guillon, *J. Vac. Sci. Technol. A*, these proceedings.
- ⁹P. Wei, S. Tixier, M. Chicoine, S. Francoeur, A. Mascarenhas, T. Tiedje, and F. Schiettekatte, *Nucl. Instrum. Methods Phys. Res. B* (in press).
- ¹⁰Z. Lin, L. C. McIntyre, Jr., J. A. Leavitt, M. D. Ashbaugh, and R. P. Cox, *Nucl. Instrum. Methods Phys. Res. B* **79**, 498 (1993).
- ¹¹F. Schiettekatte, M. Chicoine, J. S. Forster, J. S. Geiger, S. Gujrathi, R. Kolarova, A. Paradis, S. Roorda, and P. Wei, *Nucl. Instrum. Methods Phys. Res. B* (in press).
- ¹²*Handbook of Modern Ion Beam Materials Analysis*, edited by J. R. Tesmer and M. Nastasi (Materials Research Society, Pittsburgh, 1995), p. 248.
- ¹³L. R. Doolittle, *Nucl. Instrum. Methods Phys. Res. B* **9**, 344 (1985).